PRODUCTION AND CHARACTERIZATION OF MICRO-SIZE PORES FOR ION TRACK ETCHING APPLICATIONS

Antonino CANNAVO'[1], Vladimir HAVRANEK[1], Vasily LAVRENTIEV[1], Lorenzo TORRISI[2], Mariapompea CUTRONEO[1], Giovanni CECCIO[1], Alfio TORRISI[1], Pavel HORAK[1], Jiri VACIK[1]

[1]Nuclear Physics Institute of the CAS, Husinec Řež, Czech Republic, EU, cannavo@ujf.cas.cz
[2]Dipartimento di Scienze Fisiche - MIFT, Università di Messina, Messina, Italy, EU

Abstract

For many years the applications of ion track etch materials have increased considerably, like charged particles detection, molecular identification with nanopores, ion track filters, magnetic studies with nanowires and so on. Over the materials generally used as track detector, the Poly-Allyl-Diglycol Carbonate (PADC), offers many advantages, like its nearly 100 % detection efficiency for charged particle, a high resistance to harsh environment, the lowest detection threshold, a high abrasion resistance and a low production costs. All of these properties have made it particularly attractive material, even if due to its brittleness, obtaining a thin film (less than 500 μm) is still a challenge.

In this work, PADC foils have been exposed to α-particles emitted by a thin radioactive source of ^{241}Am and to C ions from the Tandetron 4130 MC accelerator. The latent tracks generated in the polymer have been developed using a standard etching procedure in 6.25 NaOH solution. The dependence of the ion tracks' geometry on the ion beam energy and fluence has been evaluated combining the information obtained through a semiautomatic computer script that selects the etched ion tracks according to their diameter and mean grey value and nanometric resolution images by atomic force microscopy.

Keywords: PADC polymer, AFM, OM, Image analysis

1. INTRODUCTION

In addition to the conventional application of the ion-track polymeric materials in detection of charged particles [1] and neutrons [2], the controlled fabrication of nanopores with specific geometries and characteristics have opened in the last decades the way to other fields of research and technology, e.g., to biosensors [3], nuclear membranes for filtration [4] to templates for nanostructure preparation [5], various industrial applications [6], filters for X-rays imaging [7], and so on [8].

One of the most important advantages of such a technology is that the shape and density of the etched tracks are two independent parameters that can be tuned according to the specific criteria demanded by the applications. In fact, several aspects do concur to the development of pores - mainly the irradiation conditions and the etching procedure that can be optimized to achieve a certain purpose.

The majority of the works present now in literature [9,10] is focused on the characterization and application of ion tracks in polyethylene terephthalate (PET). This is mainly due to the advantageous properties of PET, such as the high stability in acids, biological compatibility, mechanical hardness and high etch ratio. Nevertheless, the poly-allyl-diglycol carbonate (PADC) has also unique characteristics, e.g., the highly sensitive to ionizing particles [11] that allow to create the track-etch foils for special purpose. In fact, the experimental conditions used in this paper, namely the light elements (α, C) with relatively low energy (1 MeV - 10 MeV), would not be enough to damage effectively PET and other similar polymers. However, the wide utilization of PADC is still limited because of its brittleness that makes the manufacturing of thin foils (with a

thickness < 100 μm) a challenge. In this paper are reported first results obtained by study of etched ion tracks generated in PADC and measured by a standard optical microscopy (OM) and by an atomic force microscopy (AFM).

2. EXPERIMETAL SETUP

The PADC sheets, from Page Moudlings (Pershore), of density 1.32 g/cm^3 and thickness 750 μm, have been cut to a rectangular shape (15 mm × 25 mm).

The irradiation by α-particles and carbon ions have been carried out at the CANAM infrastructure of the Nuclear Physics Institute of CAS in Řež. The irradiations by α-particles have been performed with a thin ^{241}Am radioactive source, having a main α-peak cantered at 5.486 MeV. To change the energy of the emitted α-particles, the pressure inside the vacuum chamber has been varied in the range between 430 mbar and 20 mbar, allowing to investigate the energy range between 3.5 MeV and 5.5 MeV, respectively. The energy loss by α-particles due to the variation of the pressure has been taken into account through the SRIM code. In the simulations, the pressure has been modelled by a thin absorbing layer (of air) in front of the PADC sample whose thickness (x) is given by the residual pressure inside the chamber (P_{ch}) through the equation:

$$x = \frac{P_{ch}}{P_0} D$$

where P_0 is the pressure for standard operation condition, while D is the distance between the α-source and the PADC sample, i.e., 45 mm. For each α-particle energy, the exposition time has been kept constant (20 minutes) in order to have a constant particles density hitting the surface of the PADC sample, namely 10^4 particles/cm^2. Conversely, the exposition to carbon ions have been performed along the Ion Microprobe beamline (+10°) of the Tandetron 4130 MC. The accelerated ions have been focused and scanned on the PADC foil in a surface of 1 mm^2 by a focusing quadrupole with 1 μm lateral resolution. This methodology has allowed to keep a low ions density on the PADC surface (3×10^5 particles/cm^2) in order to reduce the pores overlapping. The analysis has been repeated at different ions energy, from 0.9 MeV up to 10 MeV using 3^+ and 4^+ charge ion state.

Before the exposition of the PADC foils to ion beams, the energy peak and the ion current have been tested using a conventional solid state detector (ORTEC Ultra series) connected to a standard spectrometric chain. As expected, and confirmed also from the SRIM simulations, the spectra related to α-particles present a widening of the energy distribution when the energy decreases. In practice, the lower energies have been obtained with the higher pressure values inside the experimental chamber. This makes an increase of the α-particles straggling that results from their interaction with the residual air molecules. However, the broadening of the energy distribution does not affect the measurements with PADC, because even if the FWHM of the particles' energy rises from 38 keV to 83 keV, the difference is still lower than the minimal energy distribution that can be observed by the analysis of the etched ion tracks in PADC using the proposed technique. On the other hand, the C-ion beam has not showed any significant change of the energy resolution (it remained below 20 keV).

After irradiations, all PADC samples have been chemically etched in 6.25 N solution of NaOH. After 2 h etching at a constant temperature of 70 ± 2 °C, the samples have been washed in distilled water, dried in air and then analysed by Optical Microscopy (OM) and Atomic Force Microscopy (AFM).

The analysis with OM have been performed using an Optika DM microscope with a CCD camera interfaced with a computer through Optika Vision Lite 2.0 software. A modular NTEGRA scanning probe microscope (NT-MDT Ltd.) has been used for the AFM study.

3. RESULTS AND DISCUSSION

In **Figure 1**, two typical pictures obtained by OM are depicted. The pictures refer to the PADC foils irradiated by 5 MeV α-particles (**Figure 1a**) and C-ions (**Figure 1b**). The pores are visible as black circles in the bright background. Their regular shape is due to the fact that the ions have hit the PADC foil orthogonally to the surface with a divergence in both cases < 5°. Each picture has a resolution of 2048 x 1536 pixel corresponding to a sample surface of 237.6 μm × 178.2 μm.

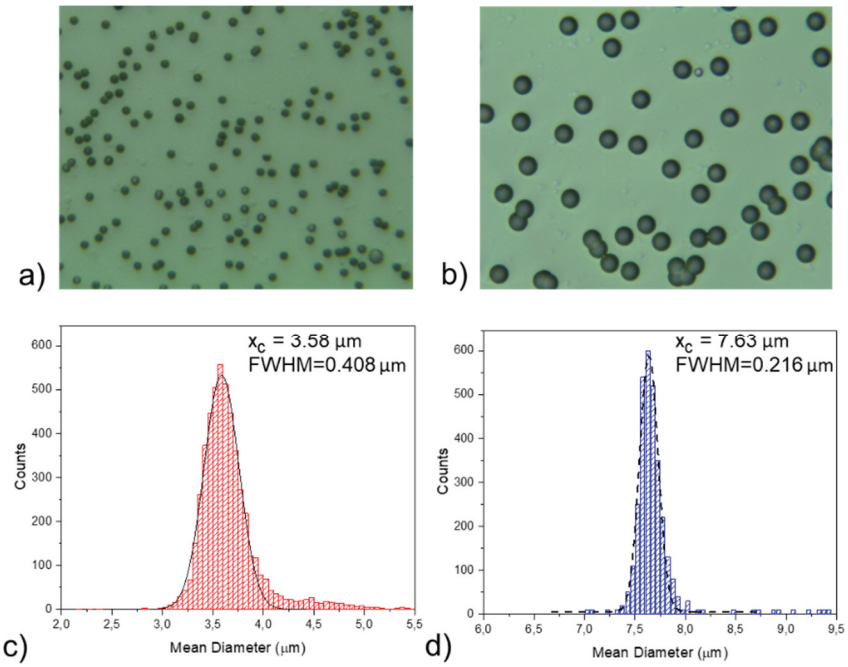

Figure 1 OM pictures of PADC foils irradiated by 5 MeV α-particles (a) and C-ions (b), and evaluation of the corresponding mean diameter (c) and (d), respectively

In order to improve the statistic of the pores (concerning the accuracy of their diameters), the sample surface has been scanned by optical microscopy and 20 pictures have been made and analysed for each sample. The pores identification has been done through an automatic script written under ImageJ environment. The selection rules of pores have been included in the script in order to select pores based on the size and shape to limit the presence of artefacts in the data analysis. These artefacts are due to several aspects, such as the overlapping of two or more pores or to a local damage of the polymer. From the counting of the total number of pores a mean density of 2.126×10^5 particles/cm^2 and 1.653×10^5 particles/cm^2 has been evaluated for α-particles and C-ions, respectively. These values are in good agreement with the ion fluences expected from the imposed experimental conditions, testifying the good efficiency of the method. Finally, standard software for the data analysis has been used to collect data from the different pictures and the pores have been classified based on area, mean gray value, major and minor axis length, position of centers, and so on. An example is depicted in the **Figure1c** and **Figure 1d** that show the evaluation of the mean diameter of pores for the samples irradiated by 5 MeV α-particles and 5 MeV C-ions, respectively. From the Gaussian fit of these data, a mean diameter of 3.58 ± 0.20 μm has been evaluated for 5 MeV α-particles, while for 5 MeV C-ions the mean diameter is 7.64 ± 0.11 μm.

Another significant example is depicted in **Figure 2**, showing how it is possible to distinguish in the same foil the pores generated by α-particles with different energies. For this purpose, a PADC foil has been irradiated twice with α-particles of 1.01 MeV and 5.48 MeV. The difference in energy determines the difference in conformation in the developed pores. In fact, the higher energy results in a mean diameter of 3.73 ± 0.19 μm,

while the lower energy produces pores with a mean diameter of 4.87 ± 0.25 μm. The pores also differ in the gray tonality (clear and dark) that reflects the different depth of the etched tracks. This aspect becomes clearer when the pore's diameter is given as a function of its mean gray value, as it is showed in **Figure 2b**. In this picture, at least two different regions can be distinguished: the first one is placed in the lower left corner that means a darker gray tonality, and it is related to the 5.48 MeV α-particles; the second area, caused by the 1.01 MeV α-particles, is positioned in the central part of the graph and has an elongate shape due to the higher broadening in the diameter distribution.

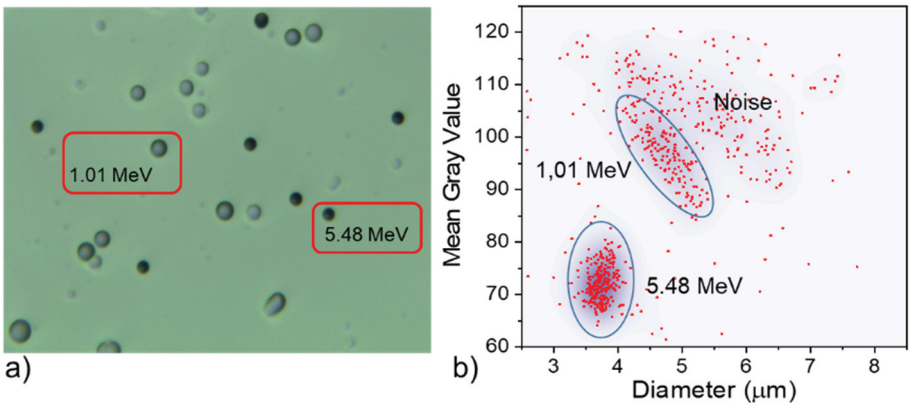

Figure 2 OM picture of a PADC sample irradiated by 1.01 MeV and 5.48 MeV α-particles, and diameter vs mean gray value of the detected pores

Following the guidelines of the OM results on the possible distribution in pores '*diameter vs. energy*', a detailed analysis of the single pores has been performed through AFM. **Figure 3a** shows the AFM picture of one of the pores of the sample already shown in **Figure 1a**.

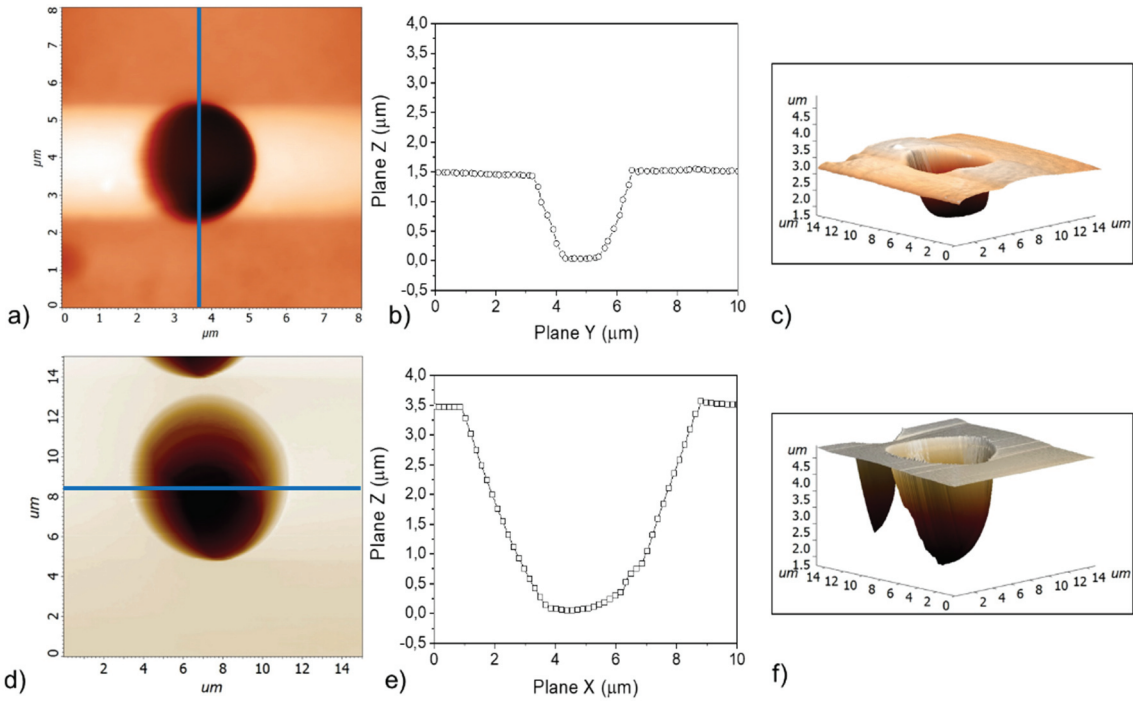

Figure 3 AFM pictures of a single pore in a PADC sample irradiated by 5 MeV α-particles a) and C-ions d), their corresponding profile analysis b) and e), and their 3D reconstructions c) and f), respectively

The profiling analysis of such a pore, **Figure 3b**, reveals a depth of 1.655 μm and confirms a diameter of 3.61 μm. The 3D reconstruction of this pore, given in **Figure 3c**, shows its conical shape. For comparison, also a pore generated by 5 MeV C-ions has been studied and the corresponding results are depicted in **Figures 3d-f**. In this case the pore has both a higher depth (3.49 μm) and a greater diameter (7.61 μm) with respect to the previous case. The same chemical etching has been done for both samples, so as expected, also in this case the pore has a conical shape, as it is showed in its 3D reconstruction in **Figure 3f**.

Combining the results carried out from OM and AFM, finally, the graphs in **Figure 4** can be obtained. Here, the dependence of the pore diameter on the particles' energy (**Figure 4a**) and the depth of the pores (**Figure 4b**) is showed. The higher energy loss of the C ions leads to a higher damage of the polymers, and this determines their faster etching rate. For this reason, at the same energy, pores related to C ions (square) have a bigger diameter and a greater depth than α-particles (circle).

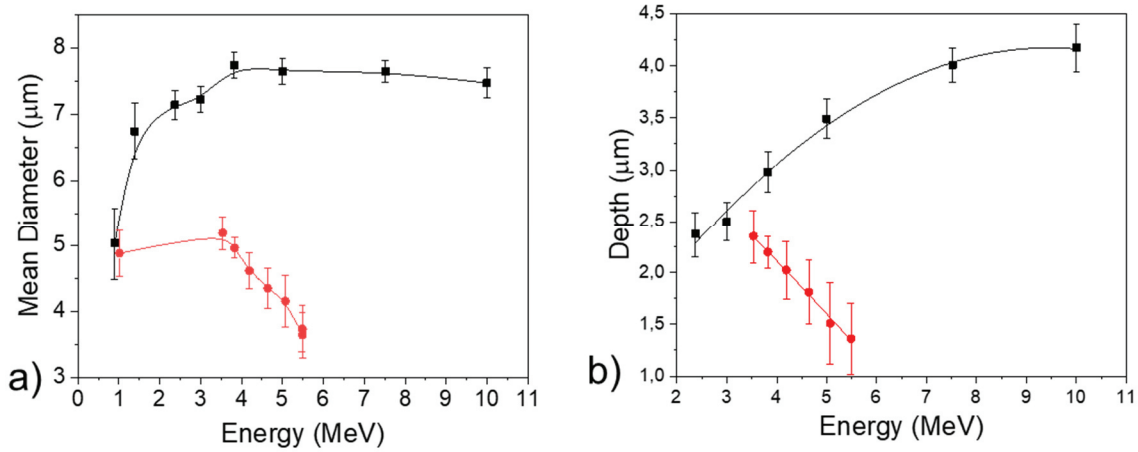

Figure 4 Dependence of the diameter and depth of the pores on energy of the α-particle (circle) and C-ions (square)

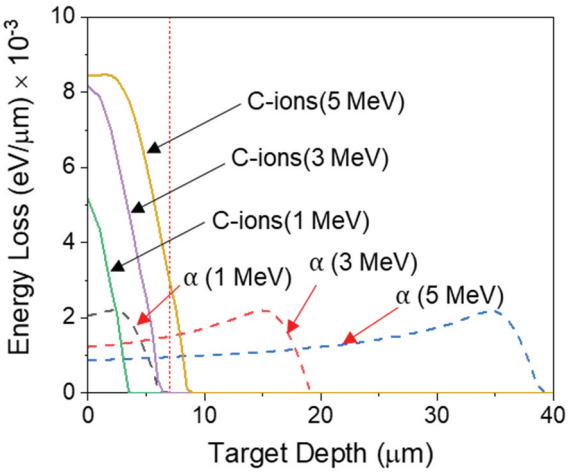

Figure 5 Energy loss for α-particles and C energy with an energy of 1 MeV, 3 MeV and 5 MeV

It should be also noted that both pictures show different trends. In the case of α-particles the mean diameter decreases quickly with the reduction of the energy, but in the case of C-ions the reduction occurs slowly. Concerning the '*depth vs energy*' dependence, the trend is totally different: when the energy increases, the pores become more/less deep in the case of C-ions/α-particles, respectively. Again, the reason of such behaviour is in the different energy loss and particles' range of the two ion species inside the PADC material.

As can been seen in **Figure 5**, α-particles have a higher range in PADC than C-ions. Consequently, α-particles lose their energy in a wider region of the sample and the Bragg peak is shifted into a deeper point of the PADC sample. For example, the range of 3 MeV α-particles in PADC, evaluated by SRIM simulation, is 18.5 μm, while for C-ions it is 5.62 μm. Considering a track etching rate of 3.5 μm/h [12], after 2 h etching the PADC foils has been etched 7 μm along the ion track path (vertical dashed line of **Figure 5**).

This means that the whole region, involved in the energy loss of C ions, can be etched out, while for α-particles the etching has not been enough to reach the Bragg peak. If the energy of the particles increases (e.g., 5 MeV) the situation for the α-particles is even worse, because the particle range becomes higher (38.2 μm) and the energy lost in the etched foil is lower. On the other hand, almost all the energy loss by the Carbon ions is included in the 7 μm etched region.

4. CONCLUSION

Encouraged by the unique properties of PADC, the characterization of the pores, etched ion tracks generated by the exposition of this plastic material to two ion species (α-particles and C ions), has been presented in the paper. The study has taken an advantage from the combination of OM and AFM study of the etched foils. Using the first technique, a large surface of the sample has been analysed. This 2D analysis has allowed to determine the '*diameter vs energy*' dependence. The latter has been used to perform the 3D AFM analysis of single pores. In such a way, a general trend has been deduced to describe also the '*depth vs energy*' dependence. OM has also permitted to distinguish between pores generated by the same type of ion (α-particles), but with two different energies (1.01 MeV and 5.48 MeV). For this purpose, the inspected pores have been classified according to the diameter and their mean gray value. The obtained data have clearly showed that the pores can be divided into distinct areas specific to given energy of ions. It should be noted that the analysis described in this paper represents a mandatory step before the introduction of PADC material to ion track-etch applications. The paper presents only preliminary results that however will be improved in the next planned experiments that will be performed using different ions (fission fragments, backscattered ions, results of nuclear reactions induced by thermal neutrons), and also with different etching parameters.

ACKNOWLEDGEMENTS

The authors acknowledge the financial support from the Grant Agency of Czech Republic under the contract No. 18-07619S. The measurements were carried out at the 'CANAM' infrastructure supported by MEYS in projects No. LM2015056.

REFERENCES

[1] MALINOWSKA, A., et al. Characterization of solid state nuclear track detectors of the polyallyl-diglycol-carbonate (CR-39/PM-355) type for light charged particle spectroscopy. *Review of Scientific Instruments.* 2014. vol. 85, no.°12, p. 123505.

[2] PUGLIESI, R., et al. Characteristics of the solid state nuclear detector CR-39 for neutron radiography purposes. *Applied radiation and isotopes*. 1999. vol. 50, no.°2, pp. 375-380.

[3] GARCÍA-ARELLANO, H., et al. Dependence of yield of nuclear track-biosensors on track radius and analyte concentration. *Nuclear Instruments and Methods in Physics Research Section B: Beam Interactions with Materials and Atoms*. 2018. vol. 420, pp. 69-75.

[4] WANG, P. et al. Ultrafast ion sieving using nanoporous polymeric membranes. *Nature communications*. 2018. vol. 9, no.°1, p. 569.

[5] MAURER, F. et al. Field emission of copper nanowires grown in polymer ion-track membranes. *Nuclear Instruments and Methods in Physics Research Section B: Beam Interactions with Materials and Atoms*. 2006. vol. 245, no.°1, pp. 337-341.

[6] APEL, P. Track etching technique in membrane technology. *Radiation Measurements*. 2001. vol. 34, no. 1-6, pp. 559-566.

[7] MITROFANOV, A.V. et al. Ion track filters in imaging X-ray astronomy. *Nuclear Instruments and Methods in Physics Research Section B: Beam Interactions with Materials and Atoms*. 2006. vol. 245, no.°1, pp. 332-336.

[8] PRICE, P. B. Recent applications of nuclear tracks in solids. *Radiation Measurements*. 2008. vol. 43, pp.S13-S25.

[9] APEL, P.Y. et al. Accurate characterization of single track-etched, conical nanopores. *Physical Chemistry Chemical Physics*. 2014. vol. 16, no.°29, pp. 15214-15223.

[10] FINK, D. et al. Coupled chemical reactions in dynamic nanometric confinement: IV. Ion transmission spectrometric analysis of nanofluidic behavior and membrane formation during track etching in polymers. *Radiation Effects and Defects in Solids*. 2015. vol. 170, no.°3, pp. 155-174.

[11] BALESTRA, S. et al. Bulk etch rate measurements and calibrations of plastic nuclear track detectors. *Nuclear Instruments and Methods in Physics Research Section B: Beam Interactions with Materials and Atoms*. 2007. vol. 254, no.°2, pp. 254-258.

[12] LOUNIS, Z. et al. Track etch parameters in CR-39 detectors for proton and alpha particles of different energies. *Nuclear Instruments and Methods in Physics Research Section B: Beam Interactions with Materials and Atoms*. 2001. vol. 179, no.°4, pp. 543-550.